Integrated In-Situ Resource Utilization System Design and Logistics for Mars Exploration

Hao Chen[a], Tristan Sarton du Jonchay[a], Linyi Hou[b], and Koki Ho[a]*

[a] *Daniel Guggenheim School of Aerospace Engineering, Georgia Institute of Technology, 270 Ferst Dr, Atlanta, GA 30313, USA,* kokiho@gatech.edu
[b] *Department of Aerospace Engineering, University of Illinois at Urbana-Champaign, 104 S. Wright St, Urbana, IL 61801, USA*
* Corresponding Author

Abstract

This paper develops an interdisciplinary space architecture optimization framework to analyze the tradeoff on in-situ resource utilization options, identify technology gaps, evaluate the benefits of in-situ resource utilization, and optimize the design of infrastructure for Mars human space exploration scenarios and mission profiles. It performs trade studies from the perspective of space logistics, which takes into account the interplanetary transportation, infrastructure deployment, in-situ resource utilization system operation, and logistics of the produced resources. Our method considers space architecture design and operation from the subsystem level to capture the coupling between in-situ resource utilization technologies and in-space architecture elements for space resource logistics. A case study involving a multi-mission human Mars exploration campaign is performed to evaluate the effectiveness of existing and proposed in-situ resource utilization technology concepts and system designs. The results can provide us with a better understanding of the benefits and costs of different in-situ resource utilization technologies for interplanetary space transportation. A sensitivity analysis is also conducted to understand the impacts of lunar and near-Earth-object's in-situ resource utilization systems on Mars missions. The results of this analysis can help decision-makers determine and optimize the roadmap for in-situ resource utilization technology development.
Keywords: Space logistics, Human space exploration, In-situ resource utilization

Nomenclature

$\mathcal{A}$	=	set of arcs
c	=	cost coefficient
d	=	mission demand
D	=	total ISRU resource demand
F	=	commodity transformation matrix
h	=	subsystem index
H	=	concurrency constraint matrix
i	=	node index
I_{sp}	=	specific impulse
j	=	node index
$\mathcal{J}$	=	optimization objective
K	=	battery/fuel cell design matrix
L	=	storage length
M	=	subsystem mass
N	=	ISRU hourly productivity
$\mathcal{N}$	=	set of nodes
P	=	subsystem power
P_0	=	power system output power
P_h	=	subsystem power demand
Q	=	infrastructure daily operating length
Q_0	=	length of a solar day
Q_p	=	length of daytime per solar day
Q_h	=	subsystem daily operating length
$\mathcal{S}$	=	total ISRU system size
t	=	time step index
$\mathcal{T}$	=	set of time steps
Δt	=	time of flight
v	=	spacecraft index
$\mathcal{V}$	=	set of spacecraft
ΔV	=	change of velocity
W	=	set of time windows
x	=	commodity variable
Z	=	ISRU daily productivity
ε	=	energy storage efficiency

Abbreviations

ISRU	=	in-situ resource utilization
FSPS	=	fission surface power system
PV	=	photovoltaic
RTG	=	radioisotope thermoelectric generator
RWGS	=	reverse water gas shift reaction
SR	=	Sabatier reaction
SOCE	=	solid oxide CO_2 electrolyzer
MRE	=	molten regolith electrolysis
HR	=	hydrogen reduction
CR	=	carbothermal reduction
SWE	=	soil/water extraction
DWE	=	direct water electrolysis
ES	=	Earth
TLI	=	trans-lunar injection
NRHO	=	near rectilinear halo orbit
PLLO	=	polar low lunar orbit
LSP	=	lunar south pole
NEO	=	near-Earth object
LMO	=	low Mars orbit
SLS	=	space launch system

EUS = exploration upper stage
CLV = commercial launch vehicle
CUS = commercial upper stage
T/V = transfer vehicle
LLAM = lunar lander ascent module
LLDM = lunar lander descent module
IMLEO = initial mass in low-Earth orbit

1. Introduction

As the interest grows in deep space exploration, large-scale space mission planning and space architecture design have become increasingly important. Both NASA [1] and SpaceX [2] have announced their exploration plans to Mars by the 2030s. To build an affordable and sustainable interplanetary space transportation system to Mars, in-situ resource utilization (ISRU) systems and propellant depots are two critical space infrastructures. They can produce and store space resources in space, especially spacecraft propellant, to support space transportation and reduce mission costs. Studies on campaign-level space mission planning have shown the effectiveness of ISRU and propellant depots for space transportation [3-7].

Multiple optimization frameworks have been proposed to perform efficient space transportation planning leveraging mission interdependencies through heuristic methods [8], simulations [9], the graph theory [10], or network flow models [3-7]. However, these methods either do not consider ISRU infrastructure design as part of the trade space or do not take into account ISRU subsystem-level interactions and trade-offs in the optimization. These interactions can directly impact the ISRU system operation mechanisms and system performances. For example, nuclear power systems, such as the fission surface power system (FSPS) and the large-scale radioisotope thermoelectric generator (RTG), can support ISRU plant continuously regardless of day and night. While the photovoltaic (PV) power system can only support the infrastructure during the daytime if no power storage system is deployed at the same time. Moreover, it also suffers from radiation degradation and dust power loss on the Martian surface. Furthermore, some ISRU processes can share the same subsystems, which makes their infrastructure design and deployment more efficient. For example, the reverse water gas shift reaction (RWGS) and Sabatier reaction (SR) processes have the same reactant (i.e., CO_2 and H_2) and both produce H_2O as one of the products. Their Martian atmosphere acquisition subsystem and H_2O storage subsystem can be designed and deployed together.

On the other hand, several testbeds have been built by NASA [11] and Lockheed Martin [12] to evaluate the performance of the hydrogen reduction reaction plant in oxygen production. Integrated prototypes were also developed for carbothermic reduction [13] and molten regolith electrolysis [14] for production demonstration. Besides the soil-based ISRU systems, Meyen [15] performed a thorough analysis of the Mars atmosphere-based ISRU experiment, also known as MOXIE. This system will be implemented on the Mars 2020 Rover for an on-site test.

Numerous studies also have been done focusing on the Martian surface transportation, resource identification and utilization assessment, and surface mission scenario analysis. Smirnova proposed a Mars surface transportation vehicle concept that guaranteed reliable flights in the Martian atmosphere [16]. Chamitoff et al. developed a powerful software tool for Martian resource identification and landing site optimization [17]. In addition, Kading et al. presented a manned Mars mission based on additive manufacturing techniques and in situ materials [18]. Do et al. conducted a detailed assessment of the Mars One mission plan [19].

However, these studies mainly focused on the standalone performance of surface systems after deployment. Our research, on the contrary, proposes an integrated ISRU design and logistics framework from an innovative perspective to take into account the relationships between surface operations and space mission planning from the subsystem-level. These relationships, which are ignored in previous literature, can directly influence mission planning solutions and ISRU infrastructure designs. For example, in space missions with frequent landing and surface operations, only a small storage subsystem is needed because most of the propellant is used right after production; whereas for space missions with low-frequency time windows because of rocket launch pad availabilities or mission demand requirements, a large storage subsystem for ISRU infrastructure is necessary.

To effectively analyze ISRU system performances, identify technology gaps, and evaluate the actual benefits of ISRU systems to human exploration to Mars, this paper proposes an interdisciplinary space architecture optimization framework that takes into account ISRU subsystem-level trade-offs and the infrastructure deployment.

There are three contributions achieved in this paper. First, the proposed architecture optimization framework enables effective space resource logistics optimization for future human exploration to Mars considering the synergistic effects of ISRU technologies, infrastructure deployment, and logistics after resource productions. Second, multiple soil-based and atmosphere-based ISRU infrastructure sizing models are established based on exiting ISRU design concepts and prototypes. These models make it possible to perform a qualitative performance comparison between different ISRU technologies. Finally, a detailed Mars exploration case study is developed based on the NASA Artemis lunar exploration architecture [20]. It is conducted to analyze

the impact of trajectory selections in Earth-Moon-Mars resource logistics and ISRU technology selections leveraging the proposed interdisciplinary space architecture optimization framework and developed ISRU sizing models.

Our method provides an important step forward in system-level architecture design and evaluation for future large-scale human space explorations. It is also particularly useful to identify the level of resource information we need to design ISRU hardware and plan space missions including the in-space transportation and landing site selection.

The remainder of this paper is organized as follows. Section 2 briefly introduces the network-based space logistics optimization method used for space mission planning. Section 3 describes the ISRU subsystem definition and infrastructure sizing models. It also covers the detailed analyses to implement power demand and supply relationships in the space mission planning formulation. In Sec. 4, model details and assumptions for human exploration to Mars are established, including candidate space transportation trajectories, the transportation network model, Martian ISRU operation environment assumptions, mission demand assumptions, and a preliminary cost model. The results and discussions are shown in Sec. 5. Finally, In Sec. 6, we conclude this paper and discuss future works.

2. Space mission planning formulation

This section introduces the network-based space logistics optimization method for space mission planning. It considers the space mission transportation model as commodity flows along arcs in a network. In this network, nodes denote orbits or planets; arcs represent trajectories; crew, payload, propellant, and spacecraft are all considered as commodities flowing along arcs. An example of the Earth-Moon-Mars transportation network model is shown in Fig. 1.

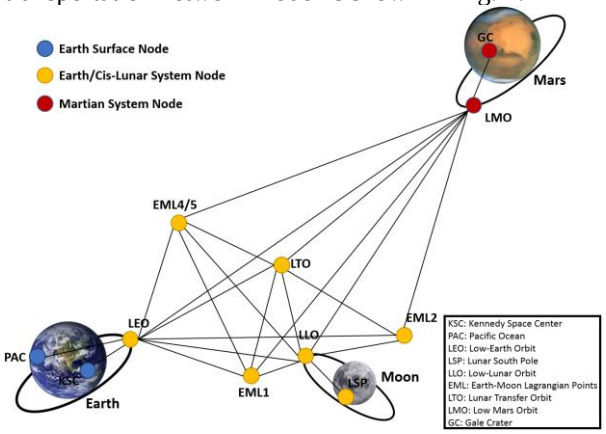

Fig. 1 Earth-Moon-Mars transportation network [7]

Consider a set of arcs $\mathcal{A}(\mathcal{V},\mathcal{N},\mathcal{T})$, which contains a set of available spacecraft $\mathcal{V}$ (index, v), a set of nodes $\mathcal{N}$ (indices, i,j), and a set of time steps $\mathcal{T}$ (index, t). To compile the space mission planning formulation, we need to define the following variables and parameters.

$\boldsymbol{x}_{vijt}$ = commodity flow variables. It can be discrete or continuous variables depending on the commodities.

$\boldsymbol{d}_{it}$ = mission supply and demand vector. Supplies are positive and demands are negative.

$\boldsymbol{c}_{vijt}$ = mission cost coefficient.

Δt_{ij} = time of flight.

F_{vij} = Commodity transformation matrix.

H_{vij} = Concurrency constraint matrix.

W_{ij} = Mission time windows.

Based on the aforementioned notations, we can express the network-based space logistics optimization formulation as follows [6].

Minimize:

$$\mathcal{J} = \sum_{(v,i,j,t)\in\mathcal{A}} \boldsymbol{c}_{vijt}{}^{T}\boldsymbol{x}_{vijt} \tag{1a}$$

Subject to:

$$\sum_{(v,j):(v,i,j,t)\in\mathcal{A}} \boldsymbol{x}_{vijt} - \sum_{(v,j):(v,j,i,t)\in\mathcal{A}} F_{vji}\boldsymbol{x}_{vji(t-\Delta t_{ji})} \le \boldsymbol{d}_{it} \quad \forall i\in\mathcal{N}\ \ \forall t\in\mathcal{T} \tag{1b}$$

$$H_{vij}\boldsymbol{x}_{vijt} \le \boldsymbol{0}_{l\times 1} \quad \forall (v,i,j,t)\in\mathcal{A} \tag{1c}$$

$$\begin{cases} \boldsymbol{x}_{vijt} \ge \boldsymbol{0}_{p\times 1} & \text{if } t\in W_{ij} \\ \boldsymbol{x}_{vijt} = \boldsymbol{0}_{p\times 1} & \text{otherwise} \end{cases} \quad \forall (v,i,j,t)\in\mathcal{A} \tag{1d}$$

$$\boldsymbol{x}_{vijt} = \begin{bmatrix} x_1 \\ x_2 \\ \vdots \\ x_p \end{bmatrix}_{vijt}, x_n \in \mathbb{Z}_{\ge 0}\ or\ \mathbb{R}_{\ge 0}\ \ \forall n\in\{1,\dots,p\} \quad \forall (v,i,j,t)\in\mathcal{A}$$

2.1 Objective function

Equation (1a) is the objective function. It can be mission cost or other mission performance measurements depending on the definition of $\boldsymbol{c}_{vijt}$.

2.2 Mass balance constraint

Equation (1b) is the mass balance constraint that makes sure the commodity inflows to a node is always larger than or equal to the summation of the commodity outflows and the mission demands. In this constraint, the second term, $F_{vij}\boldsymbol{x}_{vijt}$, represents commodity transformation during spaceflights or after infrastructure deployment, including propellant burning, crew consumptions, and ISRU resource production.

2.3 Concurrency constraint

Equation (1c) is the concurrency constraint that limits commodity flow bounds, mainly defined by the spacecraft payload capacity, the spacecraft propellant capacity, and the ISRU storage capacity. This type of constraint is also used to guarantee the non-negativity of the commodity inflows (i.e., $-F_{vij}\boldsymbol{x}_{vijt} \le \boldsymbol{0}_{p\times 1}$) l is the number of total concurrency constraint types.

2.4 Time window constraint

Equation (1d) is the time window constraint. It guarantees that only when time windows are open, commodity flows are permitted. p is the number of commodity types.

The above is a brief introduction of the space mission planning formulation through the generalized multi-commodity flow model [3-7]. For detailed constraint descriptions and constraint parameter settings, please refer to Ref. [6].

3. ISRU system modeling

This section first shows the integrated ISRU infrastructure model and modularized ISRU subsystems. Then, in Sec. 3.2, we develop a series of ISRU models by extrapolating the data from existing ISRU design concepts and prototypes. Finally, Sec. 3.3 introduces the ISRU operation models considering power system demands and landing site environments.

3.1 Integrated ISRU Infrastructure Model

There are six subsystems considered in this ISRU infrastructure model. The first subsystem is reactors, which is the core of ISRU plants. They conduct chemical processes to transform reactants into valuable products, such as water (H_2O), oxygen (O_2), hydrogen (H_2), and methane (CH_4). The sizing parameter of a reactor is the ISRU resource hourly productivity N, in the unit of kg/hr. The mass and power consumption sizing models of a reactor can be written as Eqs. (2) and (3). Note that, there are some ISRU reactors that use rigid solar concentrators to provide thermal energy to the chemical reactions, such as the integrated carbothermic reduction system [13] developed by Orbitec Inc. and NASA. For those reactors that use a special power source, we consider the power architecture as part of the reactor in the sizing model and the reactor does not require external power input anymore.

$$M_{Re} = F_1(N) \tag{2}$$

$$P_{Re} = G_1(N) \tag{3}$$

To obtain raw materials as ISRU reactants, we need the second subsystem, excavator or acquisition systems, to collect soil/regolith for the soil-based ISRU system or CO_2 for the Martian atmosphere-based ISRU system. We introduce the excavation rate $m_{Soil/Gas}$, in the unit of kg/hr, as an intermediate variable to decouple the excavation schedule and the reactor operating time. It is a function of the ISRU resource productivity N, written as $m_{Soil/Gas} = f(N)$. Based on the excavation rate $m_{Soil/Gas}$, the sizing models for excavator/acquisition subsystems can be written as Eqs. (4) and (5). The excavation complexity, difficulty, and site specificity vary depending on the target raw materials attributes. Using Mars exploration as an example, 95% of the Martian atmosphere is made up of CO_2. It is everywhere on Mars. Therefore, the reactant excavation of atmosphere-based ISRU is not a constraint for mission landing site selection on Mars. For the Martian soil-based water ISRU system, landing site selection can directly impact the ISRU performance. Granular regolith is a type of garden variety soil, which contains 1-3% water concentration. It is easy to excavate and is found in most places on Mars [21]. Gypsum/sulfate on Mars has a higher water concentration, 5-10%. However, it is a harder material that may require a rock excavator and crushing. Its locations are also limited to the equatorial region and mid-latitude area [21]. There is also subsurface ice on Mars, which requires drilling devices to collect it. The landing site for Martian icy regolith is highly selective. The design of excavator/acquisition subsystems is determined by the trade-off between the landing site and ISRU technology selections.

$$M_{Ex} = F_2\left(m_{Soil/Gas}\right) \tag{4}$$

$$P_{Ex} = G_2\left(m_{Soil/Gas}\right) \tag{5}$$

The third subsystem is separators that are used to separate products from the reactor exhaust gas. The performance and sizing of separators are directly relevant to reactor types, exhaust gas components, and operating environments. Therefore, the sizing parameter of a separator is the same as the reactor, which is the ISRU resource productivity N. The mass and power consumption sizing models of separators can be written as Eqs. (6) and (7).

$$M_{Se} = F_3(N) \tag{6}$$

$$P_{Se} = G_3(N) \tag{7}$$

The fourth subsystem is a hopper/feed/secondary subsystem, which is supporting structures for other ISRU subsystems. Therefore, its sizing is directly determined by other subsystem sizing results. To make the ISRU infrastructure design model consistent, we also use the ISRU resource productivity N as the sizing parameter. Its mass and power consumption sizing models can be written as Eqs. (8) and (9).

$$M_{HF} = F_4(N) \tag{8}$$

$$P_{HF} = G_4(N) \tag{9}$$

After resources are produced, it requires storage subsystems to temporarily store the resources before they are consumed. The capacity of storage subsystems is determined by the maximum amount of produced resources to be stored during space missions. We can define the storage length variable L, in the unit of days, then the storage subsystem capacity should be equal to QLN, where Q is the daily operating length (hr/day) and N is the ISRU hourly productivity (kg/hr). Note that, L is not the same as the total space mission duration. It is the time between two space resource logistics missions. Frequent logistics missions reduce the value of L, which decreases the capacity requirement on storage subsystems. However, frequent missions also increase

the propellant consumption and operation complexity during spaceflights. On the other hand, occasional space missions enlarge the value of L that leads to less propellant consumption in space transportation but requires larger storage subsystems to be deployed. This is a trade-off between the space logistics operation and the ISRU production operation. Based on the storage capacity QLN, its mass and power consumption sizing models can be written as Eqs. (10) and (11).

$$M_{St} = F_5(QLN) \quad (10)$$

$$P_{St} = G_5(QLN) \quad (11)$$

The last subsystem is the power subsystem, which is one of the most important subsystems in ISRU trade studies. The design and technology selections of a power subsystem are relevant to landing site choice, space mission planning, ISRU operation mechanism, and ISRU infrastructure sizing. There are mainly two categories of power sources considered in this research. The first power source is nuclear power, including FSPS and RTG. This type of power system works continuously regardless of the operating environment. Therefore, it is relatively easier to perform trade studies and system sizing analysis. The second power source is solar power, which mainly includes the PV power system whose performance is highly site-sensitive. For example, at the 0-20˚ N latitude region of Mars, the peak solar irradiance after shadowing is 450 W/ m^2 and the period of high activity for solar arrays is 6-7 hr/sol [22]. In this region, solar arrays can work through the whole year after implementing dust mitigation technologies. In the northern polar area of Mars, the peak solar irradiance after shadowing is 150 W/ m^2 and the period of high activity for solar arrays is 24.6 hr/sol [22]. However, the exploration mission can only last for about 90 days during summer in this area because of the limited solar source for the rest of the year. Moreover, if the PV power system is the main power source and ISRU systems are planned to work during the night, additional energy storage systems need to be deployed. They can be batteries or fuel cells. Different attributes of power systems and operation environments make the trade studies more complex, especially considering their interaction with space logistics mission planning. In Sec. 3.3, we will discuss how to integrate power system trade studies into the space mission planning framework. The design parameter of the power subsystem is the total power demand of all other ISRU subsystems. Then, the mass sizing model can be written as Eq. (12).

$$M_{Power} = F_6(P_{Re} + P_{Ex} + P_{Se} + P_{HF} + P_{St}) \quad (12)$$

Based on the aforementioned ISRU subsystem sizing models and their dependencies, we can combine them together and obtain an integrated ISRU modeling flow chart as shown in Fig. 2. The inputs of this integrated model are available ISRU technologies, potential power sources and the requirement of ISRU daily productivity N. The outputs are designated ISRU subsystem infrastructure designs and technology selections.

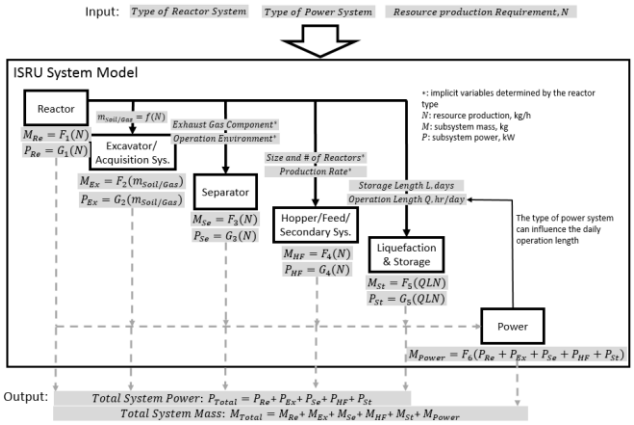

Fig. 2 Integrated ISRU modeling flow chart

3.2 Available ISRU resources

In this section, we discuss available ISRU resources and proposed ISRU sizing models. The interested resources to be produced by ISRU include water (H_2O), oxygen (O_2), methane (CH_4), and hydrogen (H_2). Table 1 shows available resources at different locations and corresponding ISRU technologies to extract these resources. These ISRU technologies are listed as follows.

Mars atmosphere based ISRU:

- Solid Oxide CO_2 Electrolyzer (SOCE)
- Reverse Water Gas Shift Reaction (RWGS)
- Sabatier Reaction (SR)
- SR/RWGS Hybrid ISRU (SR/RWGS)

Lunar soil-based ISRU:

- Molten Regolith Electrolysis (MRE)
- Hydrogen Reduction (HR)
- Carbothermal Reduction (CR)

General ISRU available for the Moon, asteroid, and Mars:

- Soil/Water Extraction (SWE)
- Direct Water Electrolysis (DWE)

Table 1 Available resources and corresponding ISRU technologies

	Moon	Mars	Asteroids
Water (H_2O)	**Resource**: Icy Regolith in Permanently Shadowed Regions (PRS) [**ISRU**: SWE]	**Resource**: Hydrated Soils/Minerals/Subsurface Icy Soils [**ISRU**: SWE]	**Resource**: Subsurface Regolith [**ISRU**: SWE]

	Resource: Minerals containing iron oxides [**ISRU**: HR (needs H_2)]	**Resource**: CO_2 in the atmosphere (~96%) [**ISRU**: RWGS (needs H_2); SR (needs H_2)]	
Oxygen (O_2)	**Resource**: Icy Regolith in Permanently Shadowed Regions (PRS) [**ISRU**: SWE/DWE] **Resource**: Minerals in Lunar Regolith [**ISRU**: MRE; CR/MR/DWE; HR/DWE]	**Resource**: Hydrated Soils/Minerals/Subsurface Icy Soils [**ISRU**: SWE/DWE] **Resource**: CO_2 in the atmosphere (~96%) [**ISRU**: SOCE; RWGS/DWE; SR/DWE]	**Resource**: Minerals in Regolith [**ISRU**: SWE/DWE]
Methane (CH_4)	**Resource**: Minerals in Lunar Regolith [**ISRU**: CR/MR]	**Resource**: CO_2 in the atmosphere (~96%) [**ISRU**: SOCE/MR (needs H_2); RWGS/DWE/MR; SR]	TBD
Hydrogen (H_2)	**Resource**: Icy Regolith in Permanently Shadowed Regions (PRS) [**ISRU**: SWE/DWE]	**Resource**: Hydrated Soils/Minerals/Subsurface Icy Soils [**ISRU**: SWE/DWE]	**Resource**: Subsurface Regolith [**ISRU**: SWE/DWE]

Table 2 ISRU infrastructure design models

System	Chemistry reactions	Reference product	Specific power, kW	Specific mass, kg
Reactor				
Solid Oxide CO_2 Electrolyzer (SOCE)	$2CO_2 \rightarrow 2CO + O_2$	O_2, kg/hr	8.64 [23]	184.23 [23]
Reverse Water Gas Shift Reaction (RWGS)	$CO_2 + H_2 \rightarrow CO + H_2O$	H_2O, kg/hr	2.4 [24]	102.3 [23, 24]
Sabatier Reaction (SR)	$CO_2 + 4H_2 \rightarrow CH_4 + 2H_2O$	CH_4, kg/hr	0.68 [23]	72.2 [24]
SR/RWGS Hybrid ISRU (SR/RWGS)	$5CO_2 + 11H_2 \rightarrow 3CO + 2CH_4 + 7H_2O$	CH_4, kg/hr	4.2 [25]	275.5 [25]
Soil/Water extraction (SWE)	$Soil \rightarrow H_2O$	H_2O, kg/hr	@3%: 13.7 [26] @5.6%: 10 [25] @8%: 7 [24]	@3%: 357 [23] @5.6%: 279 [26] @8%: 195 [26]
Direct water electrolysis (DWE)	$2H_2O \rightarrow 2H_2 + O_2$	O_2, kg/hr	5.83 [23]	83.3 [23]
Molten regolith electrolysis (MRE)	$Soil \rightarrow O_2$	O_2, kg/hr	26.94 [14]	197.58 [14]
Hydrogen reduction (HR)	$Soil + H_2 \rightarrow H_2O$	H_2O, kg/hr	0* [13, 27]	@equator: 228 [27] @pole: 482 [27]
Carbothermal reduction (CR)	$Soil + 2CH_4 + 2H_2 \rightarrow 2CH_4 + 2H_2O$	H_2O, kg/hr	0* [13,27]	520.5 [27]
Extraction/Acquisition system				
Acquisition system for CO_2	— —	CO_2, kg/hr	1.8 [23]	139.8 [23]
Excavator for soil @3% H_2O	— —	Soil, kg/hr	0.004 [28]	0.38 [28]
Excavator for soil @5.6% H_2O	— —	Soil, kg/hr	0.027 [26]	23 [26]
Excavator for soil @8% H_2O	— —	Soil, kg/hr	0.027 [26]	23 [26]
Storage system				
O_2 storage	— —	O_2, kg	0.0017 [23]	0.194 [23]
H_2 storage	— —	H_2, kg	0.0267 [29]	3.33 [29]
H_2O storage	— —	H_2O, kg	0 [29]	40 [29]
CH_4 storage	— —	CH_4, kg	0.0073 [23]	1.67 [23]
Power system				
Photovoltaic (PV) power system	— —	Power, kW	— —	6.8 (@ 1 AU) [30]
Energy storage system: battery	— —	Energy, kWh	— —	4 [31]
Energy storage system: fuel cell	— —	Energy, kWh	— —	2 [31]
Fission surface power system (FSPS)	— —	Power, kW	— —	150 [32]
Radioisotope power system (RPS)	— —	Power, kW	— —	124 [33,34]

*HR and CR reactors are integrated with rigid solar concentrators, which are their main thermal energy source

According to existing ISRU design concepts and prototypes, we develop a series of ISRU infrastructure sizing models, as shown in Table 2. The specific mass and power are the measurements of infrastructure sizing. For reactors, they mean the required system mass and power demand to generate 1 kg reference product per hour. For storage systems, they mean the necessary system mass to store 1 kg reference product. For power systems, it means the required mass to generate 1 kW power or store 1 kWh energy. This table also shows that for some ISRU technologies, the landing site environment is also a big impact factor on ISRU system performances. For example, the performances of the SWE reactor and soil excavator are different depending on the soil moisture. Moreover, due to the difference in lunar regolith composition, the performance of HR reactors is also different when deployed in the lunar equator area compared with the polar region. Furthermore, the HR and CR reactors use rigid solar concentrators as their energy source, which is considered as part of the reactors. Thus, the nominal external power demands of both HR and CR reactors are considered as zero.

3.3 ISRU Power System Trade Studies

To support ISRU subsystems, we need a power subsystem to provide enough power supply during their operations. The ISRU design model proposed in Sec. 3.2 considers the hourly productivity N as the core design variable. However, to decouple the long-time horizon mission planning from the complex ISRU internal operation tradeoffs, the daily ISRU productivity is considered as the ISRU performance criteria in space logistics optimization. ISRU daily productivity is directly determined by the power system design. In this section, we introduce the equations to consider ISRU power system design trade studies in space logistics optimization. These equations all can be categorized as concurrency constraints as shown in Eq. (1c).

3.3.1 Nuclear power system

The nuclear power system is one of the most common power sources in human space missions. We know that the ISRU infrastructures are designed based on the hourly productivity N. However, in space logistics, the transportation system cares about ISRU daily productivity Z. Now, we denote the length of a solar day at the ISRU landing site as Q_0, the daytime length in a solar day as Q_p, and the length of ISRU operation per solar day as Q. Then, the ISRU daily productivity using the nuclear power system can be written as follows:

$$Z = \max_{Q \in [0, Q_0]} QN \tag{13}$$

In Eq. (13), to maximize the ISRU daily productivity considering fixed hourly productivity, which means a fixed ISRU infrastructure design, we need to operate the ISRU for the entire solar day (i.e., $Q = Q_0$). This is to operate the ISRU system continuously throughout the space mission. Therefore, for nuclear power systems, if the ISRU power input requirement is satisfied at any specific time, the power demand of the ISRU is always satisfied throughout the entire mission. We can define a power demand vector P^{in} for ISRU subsystems and a power supply vector P^{out} for power plants. Then, define the ISRU infrastructure commodity flow variable as $\boldsymbol{x}^I$ and the power system commodity flow variable as $\boldsymbol{x}^P$. We suppose that node i is a surface node available for ISRU deployment. The nuclear power supply constraint can be expressed as Eq. (14), which has a similar format to the concurrency constraint in space logistics.

$$P^{in}\boldsymbol{x}^I_{iit} \le P^{out}\boldsymbol{x}^P_{iit} \quad \forall i \in \mathcal{N} \quad \forall t \in \mathcal{T} \tag{14}$$

3.3.2 PV power system

Aside from the nuclear power system, the PV power system is another widely used power source in space explorations. Different from nuclear power, the operating environments, especially the daytime length and the solar irradiance, have a significant impact on PV power system performances. Solar arrays can only work during the daytime. Moreover, we also need to take into account energy storage systems, such as batteries and fuel cells, that extend the ISRU daily operation length at the cost of extra mission transportation and infrastructure deployment.

Assume that we have a set of ISRU subsystems that have power demands $P_h, h \in \{1, 2, 3 \dots\}$. The daily operation length of each subsystem is denoted by Q_h. We know that we have a PV power system that can provide power P_0 during the daytime whose length is Q_p. Then, there are two scenarios regarding different ISRU subsystem operation lengths: 1) $Q_h < Q_p$; 2) $Q_h \ge Q_p$.

For the first case ($Q_h < Q_p$), given a certain level of mission demand and mission length, we want to minimize the size of ISRU infrastructures while the ISRU daily productivity (i.e., $Z_h = \max_{Q_h \in [0, Q_0]} Q_h N$) remains constant. Therefore, we want to find the maximum ISRU daily operation length Q_h for subsystem h. If there exists any ISRU subsystem h that only work during the daytime and the operation length is shorter than the daytime length, we can always extend the operation length to Q_p to achieve higher daily productivity because the solar arrays work throughout the entire daytime every solar day.

For the second case ($Q_h \ge Q_p$), because the solar arrays can only work during the daytime, we need an energy storage system to support ISRU subsystems during the night. As shown in Fig. 3, the extra energy produced by the solar arrays during the daytime (i.e., area S_1) needs to be storage and then consumed at night (i.e.,

area S_2). It can involve energy loss during the energy storage system charging and discharging. Therefore, we define an energy storage efficiency parameter, ε. Then, we get $\varepsilon S_1 = S_2$.

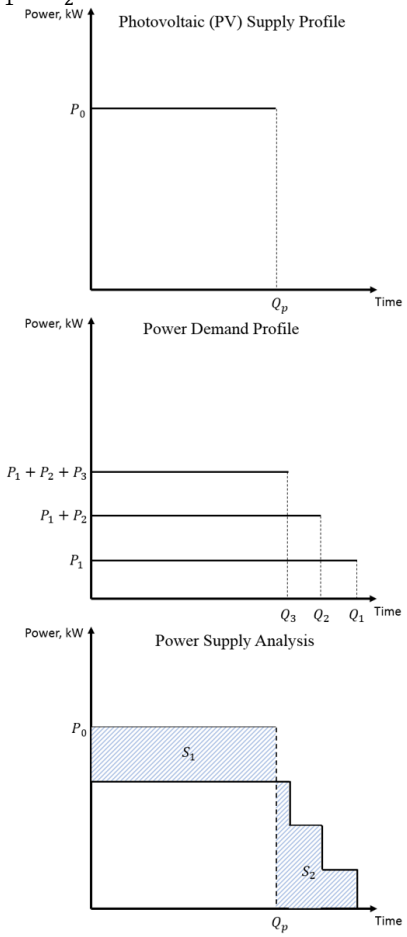

Fig. 3 PV Power Supply Analysis

Based on the power supply and demand profile in Fig. 3, we can write the energy conservation equation as Eq. (15), which means that the total energy produced by the solar arrays is equal to the summation of the energy consumed by ISRU subsystems during the daytime and the night.

$$P_0 Q_p = \sum_{h=1}^{n} P_h Q_p + \frac{\sum_{h=1}^{n} P_h (Q_h - Q_p)}{\varepsilon} \qquad (15)$$

We can rewrite the energy conservation equation as follow, where the left-hand side represents the total ISRU subsystem power demand during the daytime and the night while the right-hand side represents the total power generation of the PV power systems during the daytime.

$$\sum_{h=1}^{n} (1 + \frac{Q_h - Q_p}{\varepsilon Q_p}) P_h = P_0 \qquad (16)$$

According to the energy conservation equation shown in Eq. (16), we define an ISRU subsystem operation matrix $\mathcal{Q}$, which is a diagonal matrix. If there are n types of ISRU subsystems, it is a $n \times n$ matrix.

$$\mathcal{Q} = diag(1 + \frac{Q_1 - Q_p}{\varepsilon Q_p}, 1 + \frac{Q_2 - Q_p}{\varepsilon Q_p}, \cdots, 1 + \frac{Q_n - Q_p}{\varepsilon Q_p})$$

Then, we can write the solar power supply constraint for ISRU architecture design trade studies as follows:

$$P^{in} \mathcal{Q} \boldsymbol{x}_{iit}^{I} \le P^{out} \boldsymbol{x}_{iit}^{P} \quad \forall i \in \mathcal{N} \quad \forall t \in \mathcal{T} \qquad (17)$$

Note that if $Q_h = Q_p$ for all subsystems $h \in \{1, 2, 3 \ldots\}$, which means ISRU systems are only operated during the daytime, Eq. (17) can be simplified into Eq. (14). Moreover, based on the analysis for the first case $Q_h < Q_p$, we know that the design space of Q_h is $[Q_p, Q_0]$.

Besides the power supply constraint, we also need an energy storage system capacity constraint. We first define a battery/fuel cell design matrix K_i. Then the energy storage constraint can be expressed as Eq. (18), where the left-hand side is the total energy to be stored for ISRU night operations while the right-hand side is the total battery/fuel cell energy storage capacity.

$$\varepsilon Q_p (P^{out} \boldsymbol{x}_{iit}^{P} - P^{in} \boldsymbol{x}_{iit}^{I}) \le K_i \boldsymbol{x}_{iit}^{P,storage} \quad \forall i \in \mathcal{N} \quad \forall t \in \mathcal{T} \qquad (18)$$

3.3.3 Optimal daily operation length

Now, we have got all the necessary constraints for ISRU power system trade studies in space logistics. However, in Eq. (17), if $\mathcal{Q}$ is a design variable in the formulation, then the term $Q_h \boldsymbol{x}_{iit}^{I}$ becomes quadratic. If ISRU infrastructure design models are nonlinear, then we can solve the problem nonlinearly and this quadratic term is not an issue. But if ISRU infrastructure design models are all linear, then this quadratic term is the only nonlinear term throughout the entire formulation. It becomes valuable to perform further analysis on the optimal daily operation length before the optimization to see whether we can eliminate this quadratic term and make the entire problem to be mixed-integer linear programming.

For ISRU subsystem h, if the power system is a nuclear power system, we know that the optimal operation mechanism is to operate the ISRU subsystems continuously, which means $Q_h^* = Q_0$. In this situation, Q_h becomes a constant that only depends on the operating environment of landing sites. If the power system is the PV power system, our previous analysis shows that the optimal daily operation length Q_h^* appears in the range of $[Q_p, Q_0]$. Assume that we have a set of ISRU linear infrastructure models for ISRU subsystem h:

$$\begin{cases} Size_{ISRU} = a_1 N \\ Power_{ISRU} = a_2 N \\ Size_{PV} = a_3 P_0 \\ Size_{energy\ storage} = a_4 Energy \end{cases} \qquad (19)$$

These models are all linear functions with zero intercepts, which is consistent with the infrastructure design models as proposed in Table 2. We suppose that the total mission demands for ISRU resources are D and

the total mission length is L solar days. Then, the required hourly productivity of the ISRU system is $N = \frac{D}{Q_h L}$. We can rewrite the ISRU linear models as Eq. (20).

$$\begin{cases} Size_{ISRU} = a_1 \dfrac{D}{Q_h L} \\ Power_{ISRU} = a_2 \dfrac{D}{Q_h L} \\ Size_{PV} = a_3 Power_{ISRU}\left(1 + \dfrac{Q_h - Q_p}{\varepsilon Q_p}\right) \\ Size_{energy\ storage} = a_4 Power_{ISRU}(Q_h - Q_p) \end{cases} \quad (20)$$

For the specific mission demand and mission length, the daily operation length Q_h is the only variable in Eq. (20). We want to find the optimal daily operation length Q_h^* that minimizes the total system sizes.

$$\mathcal{S}(Q_h^*) = \min_{Q_h \in [Q_p, Q_0]} (Size_{ISRU} + Size_{PV} + Size_{energy\ storage}) \quad (21)$$

By substituting Eq. (20) into Eq. (21) and after some manipulations, we can get,

$$\mathcal{S}(Q_h) = \frac{(a_1 + a_2 a_3)D}{Q_h L} + \frac{(a_2 a_3 + a_2 a_4 \varepsilon Q_p)D(Q_h - Q_p)}{Q_h L \varepsilon Q_p} \quad (22)$$

We take a derivative of $\mathcal{S}(Q_h)$ with respect to Q_h, then we get,

$$\frac{d\mathcal{S}(Q_h)}{dQ_h} = \frac{D\left[a_2 a_3(1-\varepsilon) + a_2 a_4 \varepsilon Q_p - a_1 \varepsilon\right]}{{Q_h}^2 L \varepsilon} \quad (23)$$

In Eq. (23), the numerator of the right-hand side is always a constant after we know the ISRU infrastructure design model and ISRU landing site environment. Therefore, we can say that the system size is monotonically increasing or decreasing with respect to the ISRU daily operation length Q_h. It means that $Q_h^* = Q_p$ or $Q_h^* = Q_0$ depending on the actual ISRU design models and operating environments. Then, the entire problem can be solved linearly.

In summary, if we only consider linear ISRU infrastructure design models, for nuclear power systems, the optimal daily operation length,

$$Q_h^* = Q_0$$

For PV power systems, the optimal daily operation length,

$$Q_h^* = Q_p \text{ or } Q_h^* = Q_0$$

where the actual value of Q_h^* can be determined in advance after we know the ISRU design models and the potential landing site operation environments.

4. Human exploration to Mars: modeling and assumptions

In this section, a case study involving a multi-mission human Mars exploration campaign is developed based on the NASA Artemis lunar exploration architecture [20]. This study considers ISRU infrastructure sizing, space transportation planning, mission demand deployment, and space resource logistics concurrently. A preliminary cost model is used as the mission performance measurement.

The remainder of this section is organized as follows. Section 4.1 briefly introduces the transportation network model for the Earth-Moon-Mars transportation system and spacecraft models. Section 4.2 describes the mission demand and supply. Section 4.3 introduces mission operation assumptions and potential landing site environments for the Moon, Mars and the asteroid. Finally, Sec. 4.4 lists the cost model to evaluate the performance of space mission planning.

4.1 Mission scenario

This subsection introduces the mission scenario settings for human exploration to Mars. The mission scenario is established based on the NASA Artemis lunar exploration architecture [20]. The transportation network model is shown in Fig. 4. It is a network with eight nodes:

ES = Earth
TLI = Trans-lunar injection
NRHO = Near rectilinear halo orbit
PLLO = Polar low lunar orbit
LSP = Lunar south pole
NEO = Near-Earth object
LMO = Low Mars orbit
Mars = Mars

The trajectory ΔV and time of flight (TOF) of each arc are also shown in Fig. 4. We assume that the aeroshell is 40% of the total vehicle mass. After spacecraft land on the Martian or Earth surface, the aeroshell cannot be reused again.

There are seven different transportation vehicles/spacecraft considered in the logistics:

- SLS/EUS: exploration upper stage (mated with Space Launch System Block-1B);
- CLV/CUS: commercial upper stage (mated with Commercial Launch Vehicle);
- Mars T/V: Mars transfer vehicle;
- Orion: Orion command and service module;
- T/V: transfer vehicle;
- LLAM: lunar lander ascent module;
- LLDM: lunar lander descent module.

Each vehicle has its own designated service arcs in the network. For example, the T/V delivers LLDM and LLAM between NRHO and PLLO or helps the propellant transportation between TLI and NRHO. Except for the situation when the T/V is transported from the Earth, the flight of T/V along other arcs is not permitted. Moreover, we also assume that when enough propellant is supported, LLDM and LLAM can also flight back from PLLO to NRHO without the help of T/V. In this figure, all dash lines represent human-rated flights and solid lines represent non-human-rated flights. Note that there

is an underlying assumption in this logistics model that the spacecraft capabilities of the components can be additively combined. In reality, the interoperability between spacecraft can be significantly more complex. This assumption is also extended to spacecraft, which means the vehicle that is piggybacking on another spacecraft is treated as a payload of another spacecraft and thus does not consume its own propellant.

To simplify the analysis, the spacecraft design is not considered as part of the trade study in space logistics optimization. Instead, spacecraft with fixed design parameters are considered for space transportation. Most of the design parameters come from existing literature. Some spacecraft parameters that are not available are extrapolated based on available spacecraft design models. The spacecraft designs for this case study are listed in Table 3. Note that, launch vehicles are not considered as part of space logistics transportation. Only launch cost and payload capacities are considered for launch vehicles in mission planning.

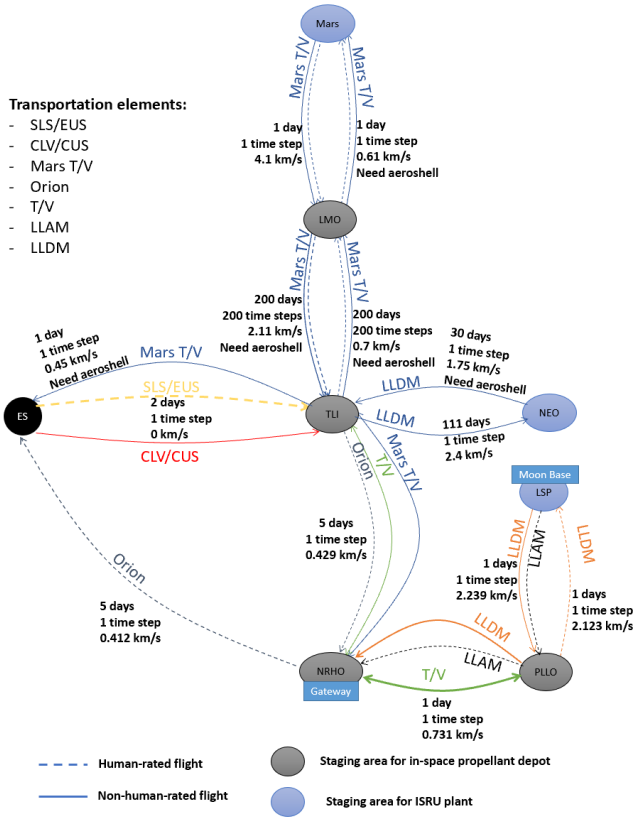

Fig. 4 Earth-Moon-Mars transportation network model

Table 3 Spacecraft design parameters

Parameter	Assumed value
SLS/EUS	
Propellant type	— —
Propellant capacity, kg	— —
Structure mass, kg	— —
Payload capacity, kg	37,000 [35,36]
Propellant I_{sp}, s	— —
Propellant component mass ratio	— —
CLV/CUS	
Propellant type	— —
Propellant capacity, kg	— —
Structure mass, kg	— —
Payload capacity, kg	18,000 [36]
Propellant I_{sp}, s	— —
Propellant component mass ratio	— —
Orion	
Propellant type	MON/MMH [37]
Propellant capacity, kg	8,915 [4]
Structure mass, kg	16,572 [37]
Payload capacity, kg	46,147*
Propellant I_{sp}, s	316 [37]
Propellant component mass ratio	— —
T/V	
Propellant type	LH2/LOX
Propellant capacity, kg	7,000**
Structure mass, kg	1,194**
Payload capacity, kg	34,864*
Propellant I_{sp}, s	420
Propellant component mass ratio	O_2: H_2=5.5:1
Mars T/V	
Propellant type	LH2/LOX
Propellant capacity, kg	7,0000**
Structure mass, kg	9,216**
Payload capacity, kg	75,000*
Propellant I_{sp}, s	420
Propellant component mass ratio	O_2: H_2=5.5:1
LLAM	
Propellant type	LH2/LOX
Propellant capacity, kg	4,800**
Structure mass, kg	3,969**
Payload capacity, kg	20,756*
Propellant I_{sp}, s	420
Propellant component mass ratio	O_2: H_2=5.5:1
LLDM	
Propellant type	LH2/LOX
Propellant capacity, kg	15,200**
Structure mass, kg	2,367**
Payload capacity, kg	136,148*
Propellant I_{sp}, s	420
Propellant component mass ratio	O_2: H_2=5.5:1

* The payload capacity is calculated based on orbital mechanics according to other spacecraft design parameters and their designated service arcs. Note that, this is just an upper bound. The actual payload capacity of a spacecraft along a specific arc is subject to the constraints from mission demand and supply, propellant capacity, and orbital mechanics concurrently.

** These design parameters (i.e., propellant capacity and structure mass) are designed based on a data-based spacecraft model developed by Taylor [38].

4.2 Mission demand and supply

The transportation mission demand and supply are assumed based on NASA DRA 5.0. The Earth-Mars transportation time window opens every 780 days. For each time window, there is a mission demand for delivering 51,700 kg payload or habitat to Mars from Earth. We assume that there is a setup phase before regular cargo transportation missions. In this setup phase, there is one time window available to deploy ISRU infrastructures on the Moon, the NEO, or Mars. There are two different mission scenarios considered in this Mars transportation mission. The first scenario is a cargo transportation mission, which is a one-way mission to deploy a certain amount of payload to Mars. Another mission scenario is a human exploration mission, which is a round-trip. Besides the cargo transportation demand, after landing on Mars for 500 days, the crew and crew cabin will come back to the Earth in the human mission. The total mission of crew and crew cabin is assumed as 20,000 kg. The mission demand and supply of Mars transportation missions are summarized in Table 4.

Table 4 Demand and supply of Mars transportation

Payload Type	Node	Demand Time, day	Supply, kg
Cargo Mission (One way)			
Payload	Earth	780*	+51,700
Payload	Mars	980*	-51,700
Payload, propellant, ISRU plant, ISRU maintenance spares	Earth	All the time	+∞
Human Exploration (Round trip)			
Payload	Earth	780*	+51,700
Payload	Mars	980*	-51,700
Crew & crew cabin	Mars	1,480*	+20,000
Crew & crew cabin	Earth	1,680*	-20,000
Payload, propellant, ISRU plant, ISRU maintenance spares	Earth	All the time	+∞

* These demands or supplies will repeat every 780 days

4.3 Mission operation assumptions

This section introduces mission operation assumptions for space mission planning, including mission time windows, ISRU maintenance requirements, landing site environment assumptions, power system degradations, crew consumptions, etc. All these assumptions and parameters are listed in Table 5. For mission time windows, we define that they are open for a few time steps after each rocket launch opportunity. Then, all space flights are prohibited when time windows are closed. Moreover, during the space mission, the ISRU infrastructure requires maintenance. The mass of necessary maintenance spares is 10% of the ISRU system mass every year. We also assume that the asteroid (i.e., near-Earth object (NEO)) has exactly the same environment as the Moon. The purpose of considering NEO ISRU is to analyze the impact of ISRU plant location on the interplanetary transportation system.

Table 5 Mission operation and landing site environment parameters and assumptions

Parameter	Assumed value
Mission Operation	
Rocket launch interval, day	780
ISRU maintenance, system mass/yr	10% [6]
PV radiation degradation, /sol	0.014% [39]
Battery charging efficiency	95% [40,41]
Fuel cell energy efficiency	60% [31]
RPS degradation rate, /yr	1.9% [33]
Food consumption rate, kg/day/person	1.015 [6]
Water consumption rate, kg/day/person	5.31 [6]
Oxygen consumption rate, kg/day/person	0.84 [6]
Mars Landing Site Environment	
Mars solar irradiance (5-20°N), kW/m^2	0.45 [22]
Regular dust power loss on Mars	5% [42]
Incident energy loss in dust storms	65% [42]
Solar day length, hr/sol	24.6 [22]
Period of operation, t_p, hr/sol	7 [22]
System mass contingency	20% [1]
Lunar Landing Site Environment	
Lunar landing site	South Pole [20]
Solar irradiance (@ 1 AU), kW/m^2	1.36 [42]
Synodic day length, day	29.5
Illumination conditions, day	27 [43]
Water ice concentration in the regolith	5.6% [44]
NEO Landing Site Environment	
Solar irradiance (@ 1 AU), kW/m^2	1.36 [42]
Synodic day length, day	29.5
Illumination conditions, day	27 [43]
Water ice concentration in the regolith	5.6% [44]

4.4 Mission cost model

To measure and analyze the impact of ISRU systems in space exploration, a cost model is needed to provide an intuitive interpretation of space mission performances.

Due to the limited data sources, we propose a preliminary cost model that is developed based on space cost estimation tools and past literature. For the high-fidelity cost model, further analysis is needed.

We assume that the total cost of space architecture is made up of system development cost, manufacturing cost/purchase price, and operation cost. The preliminary cost model is shown in Table 6.

Table 6 Preliminary cost model for Mars transportation mission

Commodities	Development cost	Manufacturing cost /Purchase price	Operation cost
SLS/EUS	— —	— —	$27,027/kg payload [36, 45]
CLV/CUS	— —	— —	$5,555/kg payload [36, 45]
Mars T/V	— —	$252M [46]	$1M/flight [47]
Orion	— —	$635M [46]	$1M/flight [47]
T/V	— —	$94M [46]	$1M/flight [47]
LLAM	— —	$211M [46]	$1M/flight [47]
LLDM	— —	$430M [46]	$1M/flight [47]
H_2O tank (1000kg*)	— —	$1.09M [48]	— —
H_2 tank (1000kg*)	— —	$4.78M [48]	— —
O_2 tank (1000kg*)	— —	$1.34M [48]	— —
DWE reactor	— —	$1,480/kg [49]	$3,000/kg system/year [48]
SWE reactor	$10,000/kg [50]	— —	$3,000/kg system/year [48]
MRE reactor	$10,000/kg [50]	— —	$3,000/kg system/year [48]
HR reactor	$10,000/kg [50]	— —	$3,000/kg system/year [48]
CR reactor	$10,000/kg [50]	— —	$3,000/kg system/year [48]
Soil excavator	$10,000/kg [50]	— —	$3,000/kg system/year [48]
SOCE reactor	$10,000/kg [50]	— —	$3,000/kg system/year [48]
RWGS reactor	$10,000/kg [50]	— —	$3,000/kg system/year [48]
SR reactor	$10,000/kg [50]	— —	$3,000/kg system/year [48]
SR/RWGS	$10,000/kg [50]	— —	$3,000/kg system/year [48]
Gas acquisition	$10,000/kg [50]	— —	$3,000/kg system/year [48]
PV (solar panels)	— —	$15,773/kg [51]	— —
FSPS (Kilopower)	$13,333/kg [32]	— —	— —
Batteries	— —	$1,000/kg	— —
Maintenance spares	— —	— —	$2,000/kg
H_2O	— —	$0.0004/kg	— —
H_2	— —	$5.97/kg [47]	— —
O_2	— —	$0.15/kg [52]	— —

*The manufacturing cost is defined for the tank with a structure mass of 1,000 kg

5. Human exploration to Mars: results and analysis

Now we have compiled a mission scenario for human exploration to Mars, considering both interplanetary cargo transportation and human exploration. This section shows the mission planning results for two different mission scenarios. Sensitivity analysis is also performed to analyze the impact of power system selections, ISRU technology selections, and lunar ISRU to Mars transportation missions. The problem is solved using the Gurobi 8.1 solver through Python on an i9-9900k, 3.6GHz platform with 32GB RAM. The detailed analysis and discussion of this human lunar exploration campaign case study are shown in the following parts. As a baseline mission scenario assumption, the FSPS is selected as the default stationary power supply system on the lunar and Martian surface; The PV power system and energy storage system are used as the default power sources in space.

5.1 ISRU technology selections

The ISRU power system comparisons between the PV system and the FSPS considering cargo transportation (i.e., one-way mission) and human exploration (i.e., round-trip mission) missions are shown in Fig. 5 and Fig. 6, respectively.

First, we can find that when considering the cargo transportation mission, the ISRU plant using the PV system has limited benefit to the space mission; whereas the ISRU plant using FSPS can provide a good mission cost saving. In the human exploration mission, which is a round-trip. Both the PV system and FSPS can provide benefits to space transportation. However, the FSPS provides a significantly larger mission cost saving by deploying a similar amount of ISRU system as in the

mission planning considering the PV system. This result shows that the FSPS is a better choice than the PV system under current mission demand and system design model assumptions.

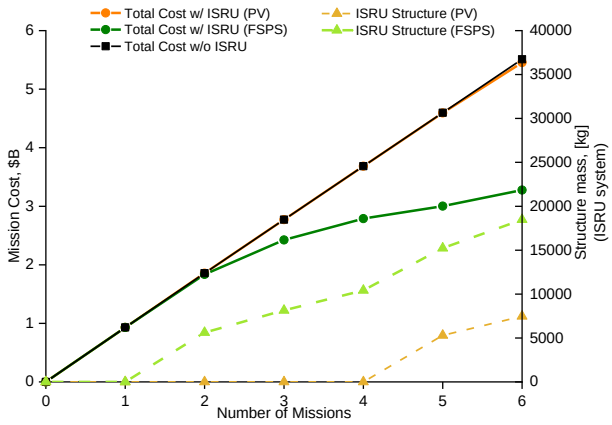

Fig. 5 Power system comparison in a cargo transportation mission

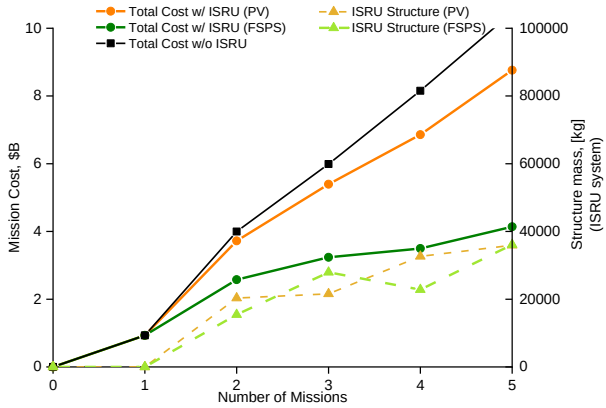

Fig. 6 Power system comparison in a human exploration mission

By fixing the ISRU power system to the FSPS, we perform a sensitivity analysis on ISRU technology selection for the human exploration mission as shown in Fig. 7. Note that, since only the LH2/LOX propulsion system is considered as the spacecraft propulsion system in the spacecraft design, some CH_4 related Martian ISRU is not taken into account in the analysis. From the result, we can find a hybrid ISRU system using SWE and HR has the best performance. It is slightly better than SWE ISRU independently, which extracts water from Martian soil and generates oxygen and hydrogen through water electrolysis. Both the SWE/HR and SWE systems are much better than other ISRU systems. Note that, even though considering a hybrid ISRU system may be economically more beneficial, technology development, plant deployment, and system operations can be significantly more complicated. Therefore, in reality, the actual mission planning decision-making process also needs to take into account other factors through comprehensive evaluations. This result shows that the proposed space infrastructure design framework is not only able to perform ISRU technology comparison but also able to consider the synergistic effect of technologies.

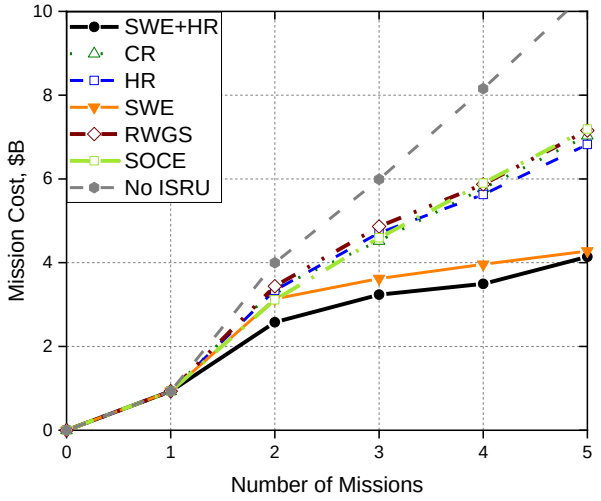

Fig. 7 ISRU technology selection in human space exploration mission, FSPS

5.2 Impact of lunar ISRU

In all results discussed above, ISRU systems are all deployed on Mars. No ISRU architecture is deployed either on the lunar surface or on the NEO. To analyze the impact of lunar ISRU on Mars transportation, we run multiple cases considering lunar ISRU deployment in the Mars transportation mission. In all the following numerical experiments, we consider a three-mission human exploration campaign to Mars. FSPS is the only power system considered in mission planning. We compare the total mission cost with respect to different amounts of lunar ISRU deployed.

First, we consider monetary mission cost as the mission planning metric using our proposed preliminary cost model. The result is shown in Fig. 8, where we also take into account the sensitivity analysis on spacecraft structure mass. We assume that because of the technology development in structure and materials science, the spacecraft structure mass may be reduced significantly in future human exploration. In this analysis, we consider the spacecraft structure mass to be 100%, 80%, and 60% of the original baseline spacecraft dry mass from the sizing model. This result shows that the deployment of lunar ISRU is not beneficial to the Mars transportation mission in this considered scenario. The reason is not that ISRU cannot provide propellant support to the Mars transportation mission. It is that the ISRU deployment cost is higher than the benefit it can provide, which means the lunar ISRU deployment cost cannot be paid off later. Fig. 9 compares the total mission

cost with or without ISRU system deployment in advance before the Mars transportation mission (e.g., for other lunar missions). If we do not consider the ISRU deployment cost, which represents the case that we have already deployed ISRU in advance during other missions, the lunar ISRU can provide propellant to support the Mars transportation mission and reduce the mission cost.

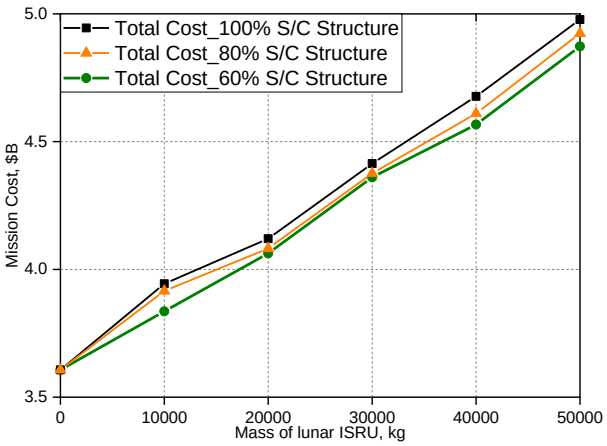

Fig. 8 Lunar ISRU impact in human exploration to Mars, monetary cost model

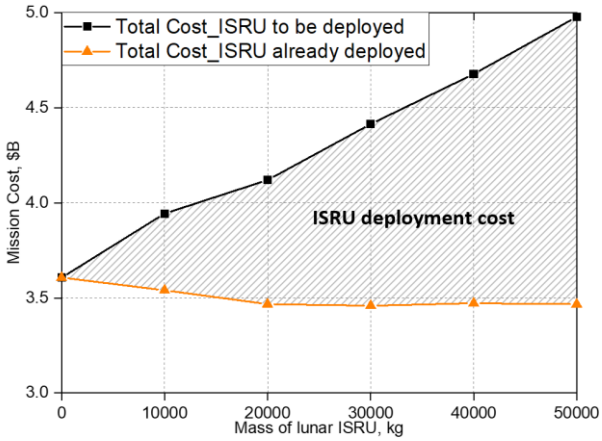

Fig. 9 Lunar ISRU impact on human exploration to Mars w/ or w/o ISRU deployment in advance

Also, the cost metric can be a key factor for the evaluation of the value of ISRU. To evaluate the influence of mission planning metrics, we conduct the same sensitivity analysis with respect to the amount of lunar ISRU deployment but using initial mass in low-Earth orbit (IMLEO) as the mission objective. The result in Fig. 10 shows that when using IMLEO as the mission cost metric, lunar ISRU can be beneficial to Mars transportation missions even when considering the ISRU deployment cost. The main difference comes from the fact that all commodities are treated in the same weight when implementing the IMLEO metric. For example, based on our cost model, the LH2/LOX propellant is less than $1 per kg; whereas the ISRU plant structure is $10,000 per kg. It is significantly more expensive to get 1 kg ISRU plant in LEO than the propellant when the monetary cost model is considered. This result shows that the analysis results depend on the cost model and assumptions.

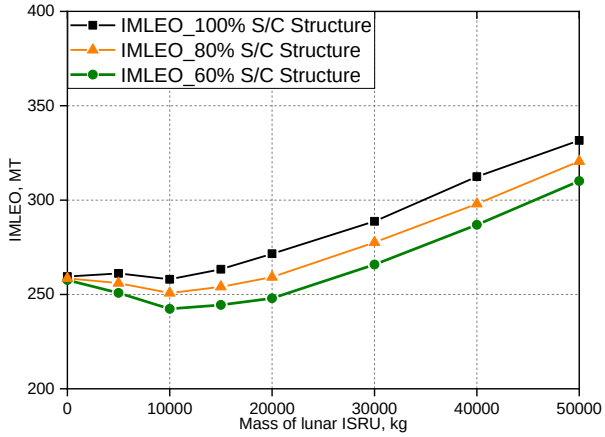

Fig. 10 Lunar ISRU impact in human exploration to Mars, IMLEO

5.3 Impact of NEO ISRU

The impact of the ISRU plant deployment location is shown in Fig. 11, where we compare the monetary mission cost for the cases in which the ISRU is deployed on the lunar surface or the NEO. Note that, in both scenarios, the Martian ISRU is also deployed and it is not influenced by the amount of lunar or NEO ISRU deployed.

The result shows the ISRU deployment on the NEO is slightly better than the deployment on the lunar surface because the NEO is closer to the TLI orbit, which is the beginning point of the Mars transportation mission. However, the ISRU deployment cost on the NEO is still not paid off later. The space mission cost considering NEO ISRU deployment is always higher than not deploying any ISRU on the NEO.

The mission cost comparisons between the scenario with or without ISRU plant deployment in advance is shown in Fig. 12. It shows the impact of ISRU deployment cost on space transportation. We can find that if there is ISRU system deployment in advance before the Mars transportation, which means the ISRU deployment cost is not considered as part of the current mission cost, the NEO ISRU is more effective than the lunar ISRU in the considered scenario. Moreover, this result also shows that no matter whether it is lunar ISRU or NEO ISRU, after the ISRU system mass reaches a certain level (i.e., 10MT~20MT in our scenarios), increasing ISRU system size does not provide higher benefit to the Mars transportation mission.

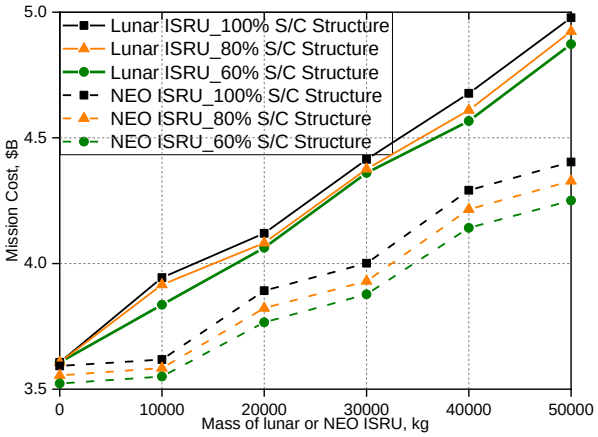

Fig. 11 Lunar or NEO ISRU impact on human exploration to Mars, monetary cost model

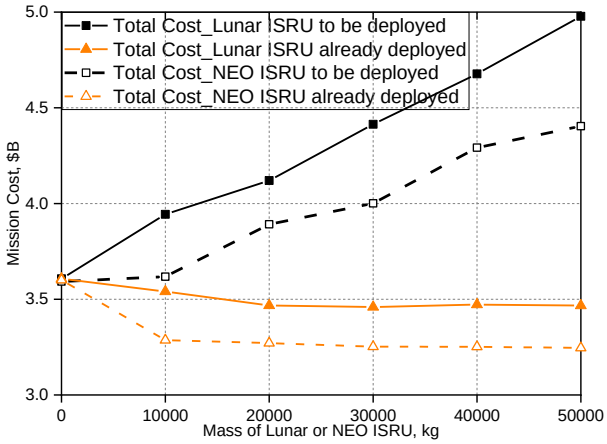

Fig. 12 Lunar/NEO ISRU impact on human exploration to Mars w/ or w/o ISRU deployment in advance

6. Conclusions

This paper proposes an interdisciplinary space infrastructure optimization framework for space resource logistics optimization in future human exploration to Mars. Multiple in-situ resource utilization infrastructure design models and cost models are developed based on existing design concepts and prototypes. A Mars exploration case study is established based on the NASA Artemis lunar exploration architecture to evaluate the performance of the proposed method and analyze the performance of in-situ resource utilization infrastructures with different technology selections. Although the numerical results can vary depending on the assumptions, the analysis shows that the proposed interdisciplinary space infrastructure optimization framework can perform in-situ resource utilization technology comparison and take into account the synergistic effect of technologies. It is also able to conduct strategic analysis considering in-situ resource utilization system deployment locations, landing site environments, available technology options, and mission scenarios.

Future research can focus on improving the computational efficiency of the proposed method for large-scale long-term space campaign design. A high-fidelity cost model is necessary to perform in-situ resource utilization infrastructure trade studies more accurately. Moreover, the current interdisciplinary infrastructure optimization method only takes into account deterministic mission scenarios for space logistics. Studies focusing on decision-making processes under stochastics mission operation environments are also important.

Acknowledgments

This material is partially based upon work supported by the funding from NASA NextSTEP program (80NSSC18P3418) awarded to the University of Illinois at Urbana-Champaign, where this work was initiated. Any opinions, findings, and conclusions or recommendations expressed in this material are those of the authors and do not necessarily reflect the views of NASA. The authors would like to thank Hang Woon Lee and Onalli Gunasekara for their reviews and thoughtful suggestions for improvement.

References

[1] B. G. Drake, Human Exploration of Mars Design Reference Architecture 5.0, NASA/SP2009-566, NASA Johnson Space Center, Houston, TX, 2009.

[2] E. Musk, Making Humans a Multi-Planetary Species, New Space, 5(2) (2017) 46-61.

[3] T. Ishimatsu, O. L. de Weck, J. A. Hoffman, Y. Ohkami, and R. Shishko, Generalized Multicommodity Network Flow Model for the Earth-Moon–Mars Logistics System, J. Spacecr. Rockets, 53(1) (2016) 25-38.

[4] K. Ho, O. L. de Weck, J. A. Hoffman, and R. Shishko, Dynamic Modeling and Optimization for Space Logistics Using Time-Expanded Networks, Acta Astronaut., 105(2) (2014) 428-443.

[5] K. Ho, O. L. de Weck, J. A. Hoffman, and R. Shishko, Campaign-level dynamic network modelling for spaceflight logistics for the flexible path concept, Acta Astronaut., 123 (2016) 51-61.

[6] H. Chen and K. Ho, Integrated Space Logistics Mission Planning and Spacecraft Design with Mixed-Integer Nonlinear Programming, J. Spacecr. Rockets, 55(2) (2018) 365-381.

[7] Chen, H., Lee, H., and Ho, K., Space Transportation System and Mission Planning for Regular Interplanetary Missions, J. Spacecr. Rockets, 56(1) (2019) 12-20.

[8] C. Taylor, M. Song, D. Klabjan, O. L. de Weck, and D. Simchi-Levi, A Mathematical Model for Interplanetary Logistics, Logistics Spectrum, 41(1) (2007) 23-33.

[9] P. T. Grogan, H. K. Yue, and O. L. de Weck, Space Logistics Modeling and Simulation Analysis using SpaceNet: Four Application Case, AIAA 2011-7346, AIAA SPACE 2011 Conference & Exposition, Long Beach, California, 2011, 27-29 September.

[10] D. C. Arney and A. W. Wilhite, Modeling Space System Architectures with Graph Theory, J. Spacecr. Rockets, 51(5) (2014) 1413-1429.

[11] K. A. Lee, L. Oryshchyn, A. Paz, M. Reddington, and T. M. Simon, The ROxygen Project: Outpost-scale Lunar Oxygen Production System Development at Johnson Space Center, J. Aerosp. Eng., 26(1) (2013) 67-73.

[12] D. L. Clark, B. W. Keller, and J. A. Kirkland, Field Test Results of the PILOT Hydrogen Reduction Reactor, AIAA 2009-6475, AIAA Space 2009 Conference and Exposition, Pasadena, CA, 2009, 14-17 September.

[13] R. J. Gustafson, B. C. White, and M. J. Fidler, 2010 Field Demonstration of the Solar Carbothermal Regolith Reduction Process to Produce Oxygen, AIAA 2011-434, 49th AIAA Aerospace Sciences Meeting including the New Horizons Forum and Aerospace Exposition, Aerospace Sciences Meetings, Orlando, FL, 2011, 04-07 January.

[14] S. S. Schreiner, Molten Regolith Electrolysis Reactor Modeling and Optimization of In-Situ Resource Utilization Systems, M.S. Thesis, Aeronautics and Astronautics Dept., MIT, Cambridge, MA, 2015.

[15] F. E. Meyen, System modeling, design, and control of the Mars Oxygen In-Situ Resource Utilization Experiment (MOXIE) and implications for atmospheric ISRU processing plants, Ph.D. dissertation, Aeronautics and Astronautics Dept., MIT, Cambridge, MA, 2017.

[16] M. Smirnova, Mars Transportation Vehicle Concept, Acta Astronaut., 103 (2014) 250-256.

[17] G. Chamitoff, G. James, D. Barker, and A. Dershowitz, Martian Resource Locations: Identification and Optimization, Acta Astronaut., 56 (2005) 756-769.

[18] B. Kading, and J. Straub, Utilizing In-Situ Resources and 3D Printing Structures for a Manned Mars Mission, Acta Astronaut., 107 (2015) 317-326.

[19] S. Do, A. Owens, K. Ho, S. Schreiner, and O. de Weck, An Independent Assessment of the Technical Feasibility of the Mars One Mission Plan – Updated Analysis, Acta Astronaut., 120 (2016) 192-228.

[20] Forward to the Moon: NASA's Strategic Plan for Lunar Exploration, 23 May 2019, https://www.nasa.gov/sites/default/files/atoms/files/america_to_the_moon_2024_artemis_20190523.pdf, (accessed 15.06.19).

[21] G. Sanders, Current NASA Plans for Mars In Situ Resource Utilization, NASA Johnson Space Center, Houston, TX, 20 February 2018.

[22] Advanced Radioisotope Power Systems Report, D-20757, Joe Parrish NASA's Office of Space Science, March 2001.

[23] G. B. Sanders, A. Paz, L. Oryshchyn, K. Araghi, A. Muscatello, D. L. Linne, J. E. Kleinhenz, and T. Peters, Mars ISRU for Production of Mission Critical Consumables - Options, Recent Studies, and Current State of the Art, AIAA 2015-4458, AIAA SPACE 2015 Conference and Exposition, Pasadena, CA, 2015, 31 August-02 September.

[24] L. Schrenk, "Development of an In-Situ Resource Utilization (ISRU) Module for the Mission Analysis Environment HabNet," M.S. thesis, MIT, Cambridge, MA, 2015.

[25] Zubrin, R. M., Muscatello, A. C., and Berggren, M., Integrated Mars In Situ Propellant Production System, J. Aerospace Eng., 26 (1) (2013) 43-56.

[26] G. B. Sanders, In-Situ Resource Utilization on Mars – Update from DRA 5.0 Study, AIAA 2010-799, 48th AIAA Aerospace Sciences Meeting Including the New Horizons Forum and Aerospace Exposition, Orlando, FL, 2010, 04-07 January.

[27] Santiago-Maldonado, E. and Linne, D. L., ISRU System Model Tool: From Excavation to Oxygen Production, Space Resources Roundtable IX, Golden, CO, 2007, 25-27 October.

[28] R. P. Mueller, J. D. Smith, J. M. Schuler, and A. J. Nick, Design of an Excavation Robot: Regolith Advanced Surface Systems Operations Robot (RASSOR) 2.0, Earth and Space 2016, 2016.

[29] D. Rapp, J. Andringa, R. Easter, J.H. Smith, T.J. Wilson, D.L. Clark, and K. Payne, Preliminary system analysis of in situ resource utilization for Mars human exploration, 2005 IEEE Aerospace Conference, Big Sky, MT, Mar. 2005.

[30] "Solar Power Technologies for Future Planetary Science Missions," JPL D-101316, Jet Propulsion Laboratory, La Cañada Flintridge, CA, Dec. 2017.

[31] "Energy Storage Technologies for Future Planetary Science Missions," JPL D-101146, Jet Propulsion Laboratory, La Cañada Flintridge, CA, Dec. 2017.

[32] "Kilopower Media Event presentation slides (May 2, 2018)", NASA, https://www.nasa.gov/directorates/spacetech/kilopower, (accessed 15.11.2018).

[33] Zakrajsek, J. F., Woerner D. F., and Fleurial J.-P., NASA Special Session: Next-Generation Radioisotope Thermoelectric Generator (RTG) Discussion, NASA, https://rps.nasa.gov/resources/69/next-generation-radioisotope-thermoelectric-generator-presentation, (accessed 15.11.2018).

[34] Schmidt, G. R., Sutliff, T. J., and Dudzinski, L. A., "Radioisotope Power: A Key Technology for Deep Space Exploration," IAC 2009, 60th International Astronautical Congress 2009, 8, (2009) 6612-6633.
[35] The Great Escape: SLS Provides Power for Missions to the Moon, https://www.nasa.gov/exploration/systems/sls/to-the-moon.html, (accessed 15.06.2019).
[36] NASA chief explains why agency won't buy a bunch of Falcon Heavy rockets, https://arstechnica.com/science/2018/03/nasa-chief-explains-why-agency-wont-buy-a-bunch-of-falcon-heavy-rockets/, (accessed 15.06.2019).
[37] Orion Quick Facts, https://www.nasa.gov/sites/default/files/fs-2014-08-004-jsc-orion_quickfacts-web.pdf, (accessed 15.06.2019).
[38] Taylor, C., "Integrated Transportation System Design Optimization," Ph.D. Dissertation, Aeronautics and Astronautics Dept., Massachusetts Inst. of Technology, Cambridge, MA, 2007.
[39] Landis, G. A., Kerslake, T. W., Jenkins, P., and Scheiman, D., Mars solar power, 2nd International Energy Conversion Engineering Conference, 1 (2004) 376-385.
[40] Toman, M., Cipin, R., Cervinka, D., Vorel, P., and Prochazka, P., Li-ion Battery Charging Efficiency, ECS Transactions, 74(1) (2016) 37-43.
[41] Parvini, Y. and Vahidi, A., Maximizing Charging Efficiency of Lithium-Ion and Lead-Acid Batteries Using Optimal Control Theory, 2015 American Control Conference, Vol. 2015-July, pp. 317-322, Chicago, IL, Jul. 2015, 01-03 July.
[42] McNatt, J., Landis G., and Fincannon, J, Design of Photovoltaic Power System for a Precursor Mission for Human Exploration of Mars, 2016 IEEE 43rd Photovoltaic Specialists Conference (PVSC), 1343-1347, Portland, OR, 2016, 05-10 June.
[43] Gläser, P., Scholten, F., De Rosa, D., Marco Figuera, R. Oberst, J., Mazarico, E., Neumann, G.A., and Robinson, M.S., Illumination Conditions at the Lunar South Pole Using High Resolution Digital Terrain Models from LOLA, Icarus, 243 (2014) 78-90.
[44] Colaprete1, A., Schultz, P., Heldmann, J., Wooden, D., Shirley, M., Ennico, K., Hermalyn, B., Marshall, W., Ricco, A., Elphic, R. C., Goldstein, D., Summy, D., Bart, G. D., Asphaug, E., Korycansky, D., Landis, D., and Sollitt, L., Detection of Water in the LCROSS Ejecta Plume, Science, 330(6003) (2010) 463-468.
[45] NASA Making Its Moon Mission Commercial Could Signal a Paradigm Shift for Deep-Space Travel, https://www.theverge.com/2019/3/15/18265417/nasa-space-launch-system-orion-em-1-commercial-space-tugs-docking-assembly, (accessed 16.06.2019).
[46] Arney, D. C., and Wilhite, A. W., Rapid Cost Estimation for Space Exploration Systems, AIAA 2012-5183, AIAA SPACE 2012 Conference & Exposition, Pasadena, CA, 2012, 11-13 September.
[47] Sowers, G., Transportation Architecture for Cislunar Space, Dec. 2015, https://www.mtu.edu/ece/department/faculty/full-time/zekavat/pdfs/ssp2015-sowers.pdf, (accessed 16.06.2019).
[48] Transportation Network Design Optimization for Cis-Lunar Space Economy (Phase II), Final Report to United Launch Alliance, 2017. https://drive.google.com/file/d/0B0rBRZHrNWuGZDBCLXlmWTZtWDA/view, (accessed 16.06.2019).
[49] Hydrogen Generator, 500mL/min. https://www.grainger.com/product/PARKER-Hydrogen-Generator-39T172, (accessed 16.06.2019).
[50] Transportation Enabling a Robust Cislunar Space Economy, ULA, Space Resources Roundtable, Planetary & Terrestrial Mining Sciences Symposium, Jun. 2016.
[51] Solar Panels, https://www.cubesatshop.com/wp-content/uploads/2016/06/ISIS-Solar-Panels-Brochure-v1.pdf, (accessed 16.06.2019).
[52] Standard Prices for Aerospace Energy Category Items, Mar. 2018, https://www.dla.mil/Portals/104/Documents/Energy/Standard%20Prices/Aerospace%20Prices/E_2018Oct1AerospaceStandardPrices_180910.pdf?ver=2018-09-10-132709-097, (accessed 16.06.2019).